# Dynamic In Situ Spectroscopic Ellipsometry of the Reaction of Aqueous Iron(II) with 2,2′-Bipyridine in a Thin Nafion Film

**Nebojša Pantelić, Chamika M. Wansapura, William R. Heineman, and Carl J. Seliskar***

*Department of Chemistry, University of Cincinnati, P.O. Box 210172, Cincinnati, Ohio 45221-0172*

*Received: March 17, 2005; In Final Form: May 25, 2005*

Dynamic in situ spectroscopic ellipsometry studies of the chemical reaction between ferrous ion and 2,2′-bipyridine (bpy) in a thin Nafion film are presented. A simple prototype system composed of a thin Nafion film on a glass substrate was used throughout the work. The reaction was detected by optically monitoring the formation of the strongly absorbing complex ion, $Fe(bpy)_3^{2+}$ ($\epsilon_{520} = 7.70 \times 10^3$ $M^{-1}$ $cm^{-1}$ in 0.1 M NaCl). The changes in film optical constants, *n* and *k*, and the thickness upon exposure of it to various solutions were monitored in a flow cell with the film on the backside of the substrate relative to the interrogation by light. A "step-by-step" approach was used to isolate the component parts of the system in which the film was consecutively exposed to solutions in the following order: supporting electrolyte, bpy, and, last, ferrous iron solution. The optical properties of the materials were quantitatively described before and during mass transport within the film by modeling using the appropriate multilayer optical models, i.e., the Cauchy equation for nonabsorbing media and the Urbach and Tauc−Lorentz (oscillator) functions for a film that absorbed. The experiments done allowed study of the diffusion in the film and the chemical reactions that are important in the sensing scheme for ferrous iron. Ligand (bpy) diffusion followed a two-stage diffusion mechanism described by a Berens−Hopfenberg model for incremental sorption ($D_{25} = 7.04 \times 10^{-13}$ $cm^2$ $s^{-1}$). The stabilities of the appropriate systems, i.e., Nafion film with bpy, iron, and iron complex, were studied by exposing equilibrated films to circulating supporting electrolyte solutions. The measurements gave important insights into a set of film chemical reactions and, in turn, selective film dynamics. This work exemplifies the usefulness of spectroscopic ellipsometry in monitoring the kinetics of a chemical reaction in situ, as well as the changes in the film physical properties under dynamic conditions.

## 1. Introduction

We have recently demonstrated spectroelectrochemical sensing of a variety of metal cations of environmental importance, and among these were aqueous $Cu^{2+}$ and $Fe^{2+}$.[1−4] In the cases of these two ions, a rather complicated sensing scheme was required for adequate sensitivity. For example, in the case of $Fe^{2+}$, the following sensor conditions had to be satisfied: (1) $Fe^{2+}$ had to partition into a chemically selective film, (2) the ion had to form a stable metal−ligand complex with a preconcentrated ligand in the film, (3) the derived $Fe^{2+}$ complex had to be oxidized or reduced at a chosen potential, and (4) the oxidized and the reduced forms of the complex had to have significantly different molar extinction coefficients at the analytical wavelength of light. The analytical signal acquired in the case of $Fe^{2+}$ was the change in absorbance between the reduced and the oxidized states of the complex, where the reduced (2+) form of the complex absorbed strongly ($\epsilon_{520} = 7.70 \times 10^3$ $M^{-1}$ $cm^{-1}$ in 0.1 M NaCl) and the oxidized (3+) form did not significantly absorb at 520 nm. Because of the success of our efforts and our interest in extending this sensing strategy from metal ions to radioactive ions, we have begun to study the more fundamental aspects of such sensing schemes by using the aqueous $Fe^{2+}$ system as a model. In doing so, we hope to better understand the dynamics of sensing in such systems, thereby becoming better able to design more dependable and robust sensors.

* Corresponding author. E-mail: carl.j.seliskar@uc.edu. Telephone: 1−513-556-9213. Fax: 1−513-556-9239.

Spectroscopic ellipsometry is a nondestructive quantitative optical technique that can determine the optical constants $n(\lambda)$ and $k(\lambda)$ of substances ($n(\lambda)$, refractive index and $k(\lambda)$, extinction coefficient, $\tilde{n}(\lambda) = n(\lambda) + ik(\lambda)$) and the thickness of thin films. Interestingly, several investigators have used spectroscopic ellipsometry in combination with electrochemistry to study electrode/electrolyte interfaces or adsorption of molecules on electrode surfaces.[5−7] In spectroscopic ellipsometry, the change in the state of polarization upon reflection of light from the sample surface is used to determine the ellipsometry parameters, $\Psi$ and $\Delta$. These two parameters are measured at each wavelength across the spectral range of interest, thus determining *n* and *k* as a function of wavelength. Previously, we have reported dynamic in situ measurements during the acid etching of indium tin oxide (ITO) films on glass substrates,[8] the partitioning of the chromophore $Ru(bpy)_3^{2+}$ into a Nafion cation-exchange thin film,[9] and the disintegration of a sensing film[10] by using spectroscopic ellipsometry. Purely optical effects on such systems caused by leaky waveguide modes of selective films have also been reported as well.[11] Taken as a whole, we have demonstrated how dynamic spectroscopic ellipsometry can be used to quantitatively track both chemical and physical changes in thin-film-based chemical sensors.

In this paper, we present new detailed studies of the $Fe^{2+}$-selective film itself using spectroscopic ellipsometry. In an effort to isolate film changes, we have again used a simple prototype system composed of a thin Nafion film on a glass substrate. Our main goal was to study the details of the metal complexation

10.1021/jp051414n CCC: $30.25 
Published on Web 06/30/2005

reaction within a thin solid sensing film. To our knowledge, there have been no previous reports of dynamic studies of in situ metal−ligand complexation reactions in a thin polymer film. Secondarily, we were better able to describe the conditions under which the sensing of aqueous $Fe^{2+}$ can be done spectroelectrochemically using a 2,2-bipyridine-loaded Nafion film.

## 2. Experimental Section

**2.1. Chemicals and Materials.** The following chemicals were used as purchased: ferrous ammonium sulfate ($Fe(NH_4)_2(SO_4)_2 \cdot 6H_2O$), Mallinckrodt), 2,2′-bipyridine (bpy, Eastman), sodium chloride (Fisher), ethanol (Fisher), and Nafion (5% solution in lower aliphatic alcohols and 10% water, Aldrich). Nafion (equivalent weight 1100) is a solubilized acid form of the polymer. On exposure to excess aqueous NaCl, the sulfonic acid groups exchange with sodium ions, giving the sodium form of the polymer. A 0.1 M NaCl solution was prepared using deionized water from a D2798 Nanopure water purification system (Barnstead, Boston, MA). Ferrous ion solution ($1 \times 10^{-5}$ M) and bpy solution ($3 \times 10^{-3}$ M) were prepared in 0.1 M aqueous NaCl. (The reader might note that we have also examined a nitrate-based supporting electrolyte for $Fe^{2+}$ sensing. Replacement of chloride by nitrate did not produce any significant changes in the results.) Solutions were delivered into the ellipsometry flow cell using Nalgene 50 silicone tubing. Solution pH values were: 6.1 (NaCl), 6.2 (bpy), and 5.9 (ferrous ion). Fine annealed SF11 and 1737F glass were obtained from Schott and Corning, respectively, and cut and polished as described previously.[9] Gaskets were cut from silicone sheeting (0.010 in. thick, gloss/gloss surface, Specialty Manufacturing, Inc., Saginaw, MI).

**2.2. Preparation of Nafion Films on Substrates.** Glass substrates were cleaned by wiping with lens paper soaked with ethanol, rinsing with deionized water, and then drying with lens paper prior to film deposition. Nafion films were then formed by first evaporating 5% Nafion stock solution to 10% and then spin-coating the resulting solution onto 1737F and SF11 glass pieces (slides) using a spin-coater (model 1-PM101DT-R485 Photo-Resist-Spinner, Headway Research, Inc.) at different spin rates (3000 and 2000 rpm, respectively) for 30 s. Coated slides were stored under ambient conditions overnight before mounting in the ellipsometer flow cell for measurements.

**2.3. Instrumentation.** Normal incidence transmission measurements were made using a Hewlett-Packard 8453 diode array spectrophotometer. A peristaltic pump (Cole-Parmer Instruments Co.) was used to circulate solutions (1.0 L volume) through the ellipsometry flow cell with a constant speed of 20 mL/min. Details of the construction of the liquid flow cell used in this study can be found in our previous work.[9] All ellipsometric measurements were made using a J. A. Woollam, Inc. variable-angle spectroscopic ellipsometer (vertical configuration). This instrument was equipped with an adjustable retarder (Auto Retarder) that enabled measurements of $\Psi$ and $\Delta$ over the full angular range (0−90° and 0−360°, respectively). The instrument also permitted depolarization of the light to be measured; however, for time-based studies, depolarization was not measured. Woollam WVASE32 software was used for optical modeling. All experiments were carried out at room temperature.

Two different scan modes were used. Static mode scans included those of glass substrates, solutions, dry films, and solution-equilibrated films. In each of these cases, the optical constants and thicknesses are invariant over time. When measuring films equilibrated with solutions, the film was exposed to circulating liquid during measurements. Static mode consisted of data acquisitions at three incidence angles, in the wavelength range 400−1000 nm at every 10 nm, with light depolarization measurements. The proper choices of angles for film interrogation are described in work by Tompkins et al.[12] An ellipsometric scan under such conditions takes far too long for a film that goes through changes in time. In such a case, the film was interrogated in dynamic mode. In dynamic mode, the scan, lasting approximately 4 min per scan, involved one incidence angle (60°) over the same wavelength range (400−1000 nm), but at every 20 nm and without depolarization measurements. The goodness of the fit of the optical model and experimental data set is expressed as a MSE value (mean square error), where MSE is the merit function.[13] All data in this study were fitted with MSE values ranging between 1 and 2. Additional details of the methods used in this work can be found in our previous publications.[8−10]

**2.4. Optical Modeling.** In the case of a selective film layer (e.g., Nafion), the optical constants and the thickness can vary significantly. Mass transport (solvent, analyte) in to and out of the film leads to changes in both $n$ and $k$ and often thickness. Indeed, it is through these changes that one is able to deduce the associated physical and chemical changes within the film. The Cauchy equation with three fitted parameters was used for data modeling (for nonabsorbing materials characterized by $k(\lambda) \cong 0$):

$$n(\lambda) = A + \frac{B}{\lambda^2} + \frac{C}{\lambda^4} \quad (1)$$

where $n(\lambda)$ is the wavelength-dependent refractive index, and $A$, $B$, and $C$ are coefficients determined through modeling experimental data. The coefficient $C$ typically has a small influence on the MSE value for ellipsometry model fitting and it was excluded from parameter fitting (Table 1S, Supporting Information). Partition of aqueous $Fe^{2+}$ into a bpy-loaded Nafion film was followed by a significant increase in optical absorbance in the range $\lambda < 700$ nm because of iron−bpy complex formation. To describe this reaction in time, it was necessary to use the complex refractive index in the fitting procedure with the associated use of oscillators (Supporting Information).

## 3. Results and Discussion

**3.1. Strategy for In Situ Measurements.** Backside film interrogation offers the opportunity to measure only the light that has interacted with the thin film.[9] Briefly, the incidence light (IL) strikes the "backside" of the glass substrate and becomes partially reflected (FR, front reflection) and refracted at the air/glass interface in accordance with Snell's law and the Fresnel equations (Figure 1). The refracted portion of the light probes the glass/film interface and once again is reflected and refracted. The light reflected at the glass/film interface, just that portion that contains information about the film (BR, back reflection), ultimately reaches the detector, and an iris at the detector can be positioned to block any other reflected beams, providing that the glass substrate is suitably thick. This configuration is appropriate for an 8-mm thick SF11 glass substrate; however, the 1737F glass used is 1 mm thick, and beam separation cannot be achieved (the actual results presented in this paper are for the SF11 glass substrate only). The beam separation is a function of the glass slide complex refractive index and thickness and incidence angle of the light.[14] A detailed description of the backside film interrogation can be found elsewhere.[9]

The sensitivity of the ellipsometric measurement is, in the first order, determined by the difference in the refractive indices

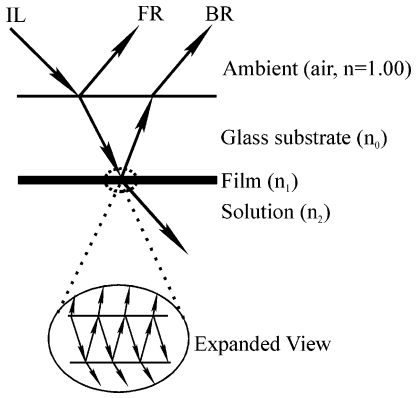


**Figure 1.** Optical scheme of the experimental setup. Backside film interrogation is demonstrated (optical layer thicknesses are not to scale).

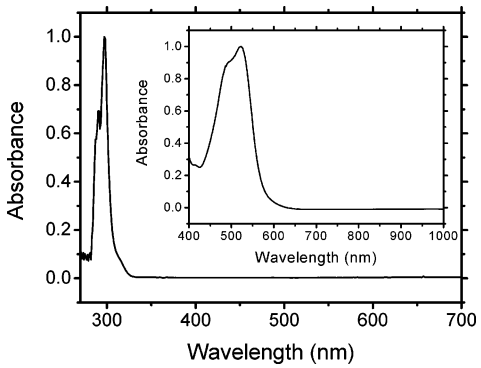


**Figure 2.** Absorbance spectrum of $1 \times 10^{-3}$ M 2,2′-bipyridine in 0.1 M NaCl solution. Inset: absorbance spectrum of $1 \times 10^{-5}$ M $Fe(bpy)_3^{2+}$ in 0.1 M NaCl solution in a wavelength range used for ellipsometric studies.

of adjacent optical layers. As a consequence, the studies in this work employed two glass substrates: a lower refractive index 1737F glass ($n_{550} = 1.517$) and a higher refractive index SF11 glass ($n_{550} = 1.792$). Identically sequenced experiments were conducted on both glass substrates to verify film results. Within an optical system composed of a solution-exposed thin-film-coated glass substrate, two important interfaces are formed: glass substrate/thin film, and thin film/solution. At the glass substrate/thin film interface, $\Delta n$ was relatively high, especially when SF11 glass was used (for a dry Nafion film on SF11, $\Delta n_{550} = 0.435$). On the other hand, Nafion has a relatively low refractive index with values close to that of aqueous solution (for a Nafion film equilibrated in 0.1 M NaCl, $\Delta n_{550} = 0.023$). Therefore, the overall sensitivity of our measurements directly related to $\Delta n$ was dominated by the film/solution interface. The distinct advantage of using SF11 over 1737F glass substrates is higher sensitivity, originating both from the larger reflected beam separation and significantly larger $\Delta n$ values.

The influence of the different solution chemical species on film properties was extracted by a stepwise experimental approach that consisted of examining the component parts of the system as we have described previously.[9] In a prototype sensing system composed of a thin Nafion film on glass that has been preloaded with the bpy ligand, one can sketch out those processes that are likely to be important in the sensing of aqueous $Fe^{2+}$:

$$\text{bpy (film)} \leftrightarrow \text{bpy (solution)} \quad \text{(a)}$$

$$Fe^{2+}\text{ (solution)} \leftrightarrow Fe^{2+}\text{ (film)} \quad \text{(b)}$$

$$Fe^{2+}\text{ (film)} + 3\text{bpy (film)} \leftrightarrow Fe(bpy)_3^{2+}\text{ (film)} \quad \text{(c)}$$

$$Fe(bpy)_3^{2+}\text{ (film)} \leftrightarrow Fe(bpy)_3^{2+}\text{ (solution)} \quad \text{(d)}$$

$$Fe^{2+}\text{ (solution)} + 3\text{bpy (solution)} \leftrightarrow Fe(bpy)_3^{2+}\text{ (solution)} \quad \text{(e)}$$

These reactions are the leaching of the bpy ligand out of the Nafion film (a), the partitioning of solution phase $Fe^{2+}$ into the Nafion film (b), the film-based complexation reaction (c), the leaching of the iron complex out of the film (d), and the complexation of solution-phase $Fe^{2+}$ with the ligand that has leached out of the film (e). On the basis of the magnitudes of the known equilibrium constants and a set of measurements that probe these reactions, the system can be described in some detail as delineated below.

**3.2. Optical Constants of Glass Materials and Liquids.** Precise determinations of the optical constants for the two types of glass substrates used were performed by ellipsometric data acquisition at several angles, followed by transmittance measurements at normal incidence. Transmittance values allowed us to determine the extinction coefficients for glass substrates below 450 nm by simultaneously fitting ellipsometric data using the Cauchy equation (sensitive to $n$) and transmission data (sensitive to $k$) using the Urbach equation[13] (Supporting Information). The optical constants of low-concentration solutions prepared in water as a solvent might be exchanged in the model for the constant of water in many practical cases. However, we found this assumption to result in relatively large errors (e.g., because of strong bpy absorption in the UV wavelength region, Figure 2), even if our studies involved very low concentration solutions. We used a previously characterized planar SF11 glass substrate for measurements on liquids using a similar experimental configuration to that of Tiwald et al.[15] Water optical constants were determined and compared very favorably with Palik's data[16] (Table 1S, Supporting Information).

**3.3 Nafion Films Equilibrated with Solutions.** The curves in panels A and B of Figure 3 are experimentally determined (solid lines) and theoretically generated (circles) $\Psi$ and $\Delta$ angles vs wavelength at 60° incidence angle for Nafion films equilibrated in various solutions obtained in static mode, respectively. The obvious conclusion from Figure 3 is that the agreement between experimental and theoretical model data is exceptionally good. In turn, that suggests that the optical-model-generated thicknesses and optical constants are essentially correct. The small near constant offset observed between the two data sets for $\Delta$ for Nafion equilibrated in 0.1 M NaCl (Panel B, curve 1) would indicate that some optical layer of very minor importance was not described adequately. This discrepancy was probed with an alternative model; the uniform optical-layer model represented in Figure 3 and used throughout the whole of this work was exchanged for a graded-layer model where optical constants were allowed to vary across the layer (film) thickness. A very small and insignificant improvement in MSE values was gained in the case of Nafion films equilibrated in NaCl. For the same film in bpy and $Fe^{2+}$ solutions, the graded-layer model resulted in significantly worse fits for the optical constants. The conclusion to be made is that within experimental error a uniform (isotropic) layer model is adequate. This result is in agreement with our previous results for Nafion films.[9]

Spectroscopic ellipsometry in the UV−vis wavelength region is unable to probe Nafion physical-chemical structure on the scale of a few angstroms as would be required to probe the finer details (charge clusters, etc.). In our previous work,[9] we established that ellipsometric data demanded a model that was isotropic or uniform in complex refractive index. Thus, we can

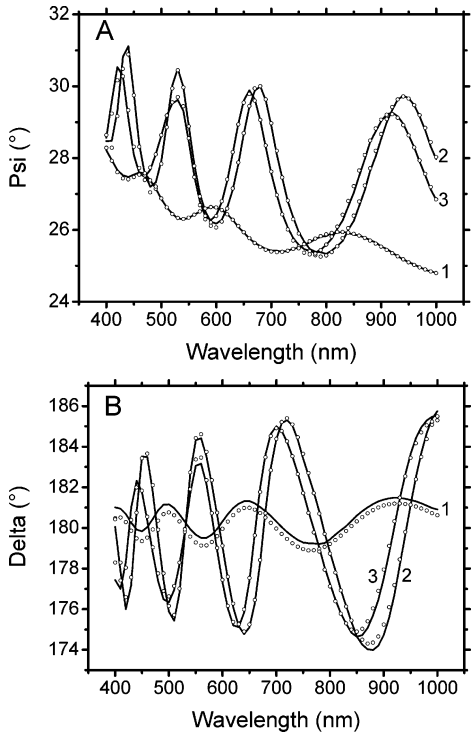


**Figure 3.** Experimentally (solid lines) and theoretically (circles) determined Ψ (Panel A) and Δ (Panel B) values at 60° incidence angle for the Nafion film equilibrated in 0.1 M NaCl (1), $3 \times 10^{-3}$ M 2,2′-bipyridine in 0.1 M NaCl (2), and $1 \times 10^{-5}$ M $Fe(bpy)_3^{2+}$ in 0.1 M NaCl (3) solutions.

say nothing about Nafion microstructure per se. The main goal of this work was to study the details of in situ metal−ligand complexation, using a well-studied ion-exchange material, and one for which we had a good ellipsometric model.

The details of the ellipsometric spectra in Figure 3 offer strong support for the chosen optical model. General rules for ellipsometry spectra are: an increase in the refractive index of an optical layer of constant thickness increases the offset of Ψ/Δ angles; an increase in layer thickness with constant refractive index red-shifts the interference maxima.[13] Comparing NaCl solution equilibrated Nafion to bpy solution equilibrated Nafion, a large increase in the offset and a red-shift in the curves was observed. In turn, this indicates both film swelling (thickness increase) and an increase in the refractive index of the film. Comparing bpy-equilibrated Nafion to $Fe(bpy)_3^{2+}$ loaded Nafion, a small blue-shift and a decrease in offset are observed. In turn, one concludes that the film has shrunk (thickness decrease) and that the overall refractive index has decreased. These same sequences are quantified from the constants of the quantitatively fitted optical model.

*3.3.1. Film Equilibrated in 0.1 M NaCl Solution.* After a dry Nafion film was fully characterized (parameters on SF11 substrate: dry film 767-nm thickness, no surface roughness, refractive index for the Nafion film $n_{550} = 1.358$, film thickness nonuniformity 5%), 0.1 M NaCl solution was injected into the flow cell. The thickness of the sodium chloride solution (and other solutions in these studies) was left as an infinite optical layer in the model with an extinction coefficient of $10^{-9}$ as necessary for proper software functioning. Nafion film responded to this bolus of salt solution by expanding by 33% with a short response time. The exact time cannot be determined with the present spectroscopic ellipsometer, but certainly this was less than one scan cycle (∼4 min). In turn, the refractive index of Nafion decreased proportionally with the amount of liquid in the polymer, i.e., as is consistent with the Bruggeman effective medium approximation[13] with 33% 0.1 M NaCl content. Equilibration of a dry Nafion film in aqueous NaCl leads to a reduction in the film refractive index, and this reduction is a superposition of two opposing contributions: a decrease in the refractive index caused by polymer hydration and a slight increase in the index caused by proton/cation exchange. The prevailing decrease in the index is due to the overwhelming contribution from polymer hydration. In comparison, a static scan after equilibration gave the following parameters for Nafion: thickness 1020 nm, $n_{550} = 1.350$.

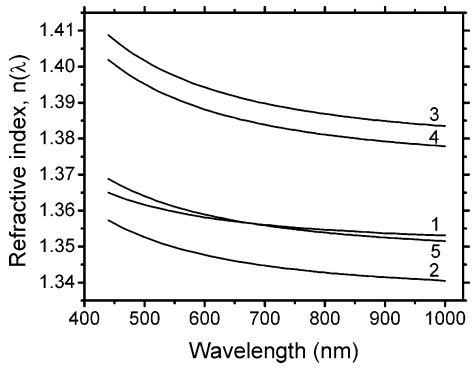


**Figure 4.** Refractive index $n(\lambda)$ vs wavelength for the dry Nafion film (1) and films equilibrated in 0.1 M NaCl (2), $3 \times 10^{-3}$ M 2,2′-bipyridine in 0.1 M NaCl (3), bpy-loaded film in 0.1 M NaCl (4), and in $1 \times 10^{-5}$ M $Fe^{2+}$ (5) solutions. The soaking solutions were again injected into the flow cell one after another.

*3.3.2. Film Equilibrated with bpy in NaCl Solution and the Stability of bpy-Loaded Nafion.* The retention of bpy by Nafion was tested in a separate experiment where a fresh Nafion film was exposed to a sequence of different solutions starting with a dry film. The results are shown in Figure 4 in the form of $n(\lambda)$ versus $\lambda$ plots. Curve 1 shows the refractive index of a dry Nafion film; curve 2, equilibrated with circulating NaCl solution; curve 3, equilibrated with circulating bpy solution; curve 4, the preloaded bpy-Nafion film reequilibrated with circulating NaCl solution; curve 5, a fresh film equilibrated with a circulating aqueous ferrous ion.

Equilibration of a dry film with NaCl solution resulted in a refractive index decrease certainly caused by film hydration and ion exchange. Equilibration of this film with aqueous bpy resulted in a large index increase. Reequilibration of the bpy-loaded film with aqueous NaCl resulted in a small decrease in the index of the film as some bpy leached out of the film. It is interesting that this equilibration caused a slight film thickness decrease (∼1%). It is important to note that the amount of leaching was small and can be estimated by comparing heights on the $n(\lambda)$ axis at an arbitrarily chosen wavelength. We estimate it to be only about 13%. Thus, it is clear that bpy is strongly retained in the Nafion polymeric matrix.

*3.3.3. Film Equilibrated in $Fe^{2+}$ in NaCl Solution.* In a repeated experiment, a fresh dry film equilibrated in 0.1 M NaCl solution was reequilibrated in ferrous ion solution (Figure 4, curve 5). It is interesting to compare $n(\lambda)$ for the curves 1, 2, and 5 in the same figure. Equilibration in ferrous ion solution resulted in a significant film refractive index increase. The ion exchange of $Fe^{2+}$ for $Na^+$ resulted in no significant thickness change. One might expect this from two opposite effects that apparently have net zero result: increase in film thickness caused by smaller ion exchange and thickness decrease caused by electrostatic cross-linking.

**3.4. Dynamic In Situ Ellipsometry.** Having determined the optical characteristics of the materials and films under static

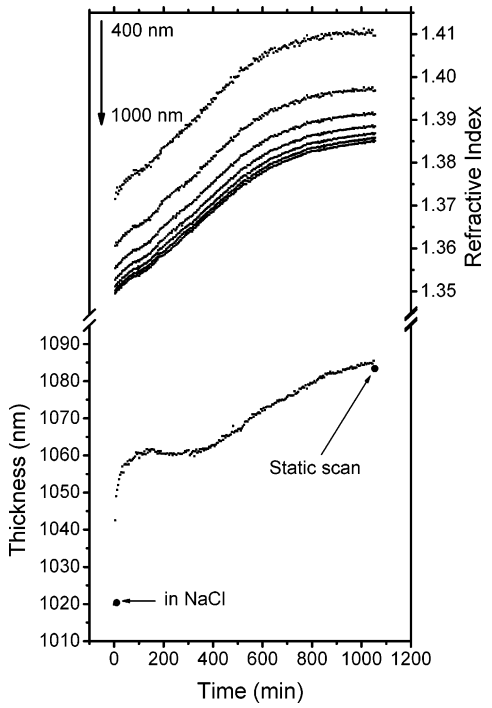


**Figure 5.** Upper graph: film refractive index at selected wavelengths (100 nm intervals) vs time for soaking of the Nafion film in $3 \times 10^{-3}$ M 2,2′-bipyridine. The film was previously equilibrated in 0.1 M NaCl solution. Lower graph: associated dynamics of the film thickness change in time.

mode conditions, we then studied the dynamics of films as detailed below.

*3.4.1. Equilibration in $3 \times 10^{-3}$ M 2,2′-Bipyridine in NaCl Solution.* After a film was fully equilibrated in aqueous NaCl, a $3 \times 10^{-3}$ M bpy solution containing 0.1 M NaCl was injected into the flow cell. The concentration of bpy was chosen in agreement with our previously described static studies. The upper curves in Figure 5 show the dynamics of the film refractive index, over the wavelength range 400−1000 nm at 100 nm intervals, where a linear functionality can be seen for approximately the first 600 min with a somewhat slower increase and leveling off in the last several hundred minutes. (The reader might note that *n*-values omitted in Figure 5 for the film equilibrated in NaCl are well below the first points shown.) The magnitude of the refractive index increase was the highest at 400 nm because of the proximity of the bpy strong UV absorption band, and it decreased systematically at longer wavelengths (all data not shown). Interestingly, different dynamics were observed for the film thickness increase (lower curve). Initially, the increase in film thickness was very fast but then leveled off for about 300 min. Starting at about the 400-minute mark, the film thickness increased again but at a much slower rate than it showed initially.

The near linear increase in the refractive index over the time interval 0−600 min offers strong evidence of continuous bpy partitioning during film equilibration. On the other hand, the film thickness dynamics showed a more complicated behavior during this same time interval. We explored this interesting behavior from a more fundamental aspect. Whereas the diffusion of a penetrant molecule in rubbery polymers is usually considered to be Fickian, glassy polymers like Nafion readily exhibit non-Fickian or anomalous behavior. This difference is thought to be caused by the varying response of the polymer structure to penetrants; rubbery polymers respond rapidly, while glassy polymers tend to respond over a longer time. Diffusion of small molecules into the glassy polymers is usually associated with a change in internal polymer structure, which is frequently attributed to the finite rate of relaxation times of individual networks that cause this anomalous behavior.

The solution of the diffusion equation for a plane film on a solid support as shown by Crank and Filipov is:[17,18,19]

$$\frac{M_t}{M_\infty} = 1 - \frac{8}{\pi^2}\sum_{n=0}^{\infty}\frac{1}{(2n+1)^2}\exp(-(2n+1)^2 k_f t) \qquad (2)$$

where $M_t$ and $M_\infty$ are the masses of the penetrant at time $t$ and at the infinite time (equilibration), respectively, and $k_f$ is the appropriate rate constant of diffusion. This last value depends on diffusion coefficient and film thickness:

$$k_f = \frac{\pi^2 D}{4{d_0}^2} \qquad (3)$$

where $D$ is diffusion coefficient and $d_0$ is initial film thickness. The diffusion constant, in turn, depends on the film thickness change, which can be corrected for solvent volume fraction, $f_{w,\infty}$:[17,19]

$$D = D^f(1 - f_{w,\infty}) \qquad (4)$$

It can be shown that, for short times, the left part of eq 3 is a linear function of $t^{1/2}$, and for longer times, the function levels off.[17−19] In a typical ellipsometric experiment, the changes of thickness and refractive index are measured in time. The following equation can be written for normalized film mass and thickness that is generally valid for all cases except those that can cause polymer shrinking caused by network cross-linking (i.e., diffusion of polyvalent ions into monovalent ion-exchange polymers):[18,19]

$$\frac{M_t}{M_\infty} = \frac{d_t - d_0}{d_\infty - d_0} = \tau \qquad (5)$$

where $d_t$, $d_0$, and $d_\infty$ are the film thicknesses at time $t$, time $t = 0$, and equilibrated film, respectively, and $\tau$ is the normalized thickness corresponding to the ratio of these quantities. Figure 6A is a plot of normalized thickness $\tau$ (squares) determined experimentally versus $t^{1/2}$ for the Nafion film during the exposure to bpy in 0.1 M NaCl solution. The solid curve represents a calculated two-stage response for the diffusion mechanism. Berens and Hopfenberg[20] developed a semiempirical model that accounts for two-stage film swelling consisting of penetrant Fickian diffusion and polymer network relaxation. The initial Fickian diffusion component involves penetration into free-volume sites like holes and voids, whereas the slower relaxation process involves redistribution of internal polymeric structure, resulting in new free-volume sites and additional penetration. The numerical model is specifically a superposition of ideal Fickian diffusion and several relaxation terms. For the plane film on the solid support, it can be written:[19,20]

$$\frac{M_t}{M_\infty} = F_f\left(1 - \frac{8}{\pi^2}\sum_{n=0}^{\infty}\frac{1}{(2n+1)^2}\exp(-(2n+1)^2 k_f t)\right) + \sum_i F_{ri}(1 - \exp(-k_{ri}t)) \qquad (6)$$

$$F_f + \sum_i F_{ri} = 1$$

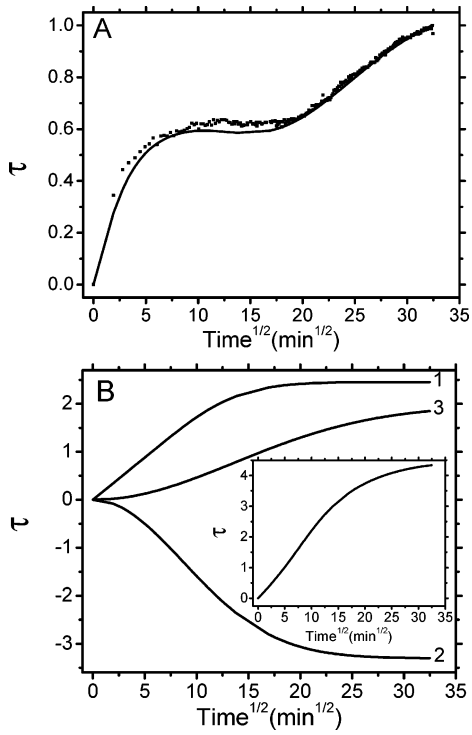


**Figure 6.** Panel A: the experimental (squares) and generated (solid line) $\tau = M_t/M_\infty$ vs $t^{1/2}$ data plot for $3 \times 10^{-3}$ M bpy uptake into Nafion film preequilibrated in 0.1 M NaCl solution. Panel B: the generated data plot for the individual terms in the eq 6; Fickian diffusion (curve 1), water desorption-first relaxation (curve 2), and second relaxation (curve 3). Inset: the sum of curves 1 and 3 presenting bpy diffusion.

**TABLE 1: Initial and Computer-Generated Parameters in the Berens−Hopfenberg Model**

| | initial | generated |
|---|---|---|
| $d_0$ (nm) | 1019 | 1021 |
| $F_f$ | 0.6 | 2.45 |
| $k_f$ (min$^{-1}$) | 0.14 | 0.01 |
| $F_{r1}$ | −0.68 | −3.3 |
| $F_{r2}$ | 1.35 | 1.96 |
| $k_{r1}$ (min$^{-1}$) | $3.2 \times 10^{-3}$ | $6.6 \times 10^{-3}$ |
| $k_{r2}$ (min$^{-1}$) | $1.4 \times 10^{-3}$ | $2.7 \times 10^{-3}$ |

where $k_{ri}$ is the first-order relaxation rate constant, and $F_f$ and $F_{ri}$ are the fractions of the contributions of Fickian diffusion and relaxations, respectively, whose sum equals unity. Two relaxation terms are usually necessary for an adequate description of the diffusion process, as was demonstrated by Berens and Hopfenberg.[20] They showed that the model is also suitable for incremental sorption (sorption that involves a finite initial penetrant or solvent concentration) involving an initial maximum followed by temporary desorption and later resorption.

We used the same model and an appropriate algorithm to fit our experimental data presented in Figure 6. The total number of seven parameters, six from eq 6 and an initial film thickness, were used as fitting variables. The initial values were chosen by intuitive inspection of the experimental curve and by trial-and-error probing. The data were optimized by minimizing the least-squares residuals. Visual comparison of the experimental curve (squares) and fitted curve (solid line) in Figure 6 reveals excellent agreement between the two sets of data. The initial and computer fitted final parameters are shown in Table 1. During fitting, the initial film thickness does not change significantly as was expected. The comparison of the rate constants gives insight into the time-resolved events. The ideal Fickian diffusion is the fastest process dominating the 1 order of magnitude slower two relaxations. All are superimposed to yield the overall curve. The sum of the fractional coefficients is close to unity as required by the model. The calculated bpy diffusion constant in the Nafion film preequilibrated in 0.1 M NaCl was $D_{25} = 4.22 \times 10^{-15}$ m$^2$ min$^{-1}$ ($7.04 \times 10^{-13}$ cm$^2$ s$^{-1}$). The magnitude of $D$ indicates a relatively slow bpy diffusion within the polymer, but the value should be taken with some caution because of model limitations.[19] Similar magnitudes of diffusion coefficients for charged metal−bpy-based compounds within Nafion film were found by the other authors ($\sim 10^{-10} - 10^{-12}$ cm$^2$ s$^{-1}$).[21−23] Moreover, it was found that the metal−ligand diffusion rate depends on the nature of the counterions present in the polymer network.[24] The first relaxation fractional coefficient has a negative value; we found this was necessary for obtaining the segment of the experimental curve with near-zero slope. In turn, this would indicate that some event that occurs during the course of bpy diffusion caused desorption, as was predicted by the Berens−Hopfenberg model in the case of incremental sorption. Prior to bpy inclusion, we did equilibrate the Nafion film in 0.1 M NaCl solution; therefore, the sorption in our case may also be thought of as fractional. In this regard, Shi and Anson[25] studied desorption of previously fully hydrated Nafion films induced by different cations, among them $Os(bpy)_3Cl_2$ and $Ru(bpy)_3Cl_2$, by using a quartz crystal microbalance (QCM). In the case of $Ru(bpy)_3^{2+}$ penetration, they found that the net increase in the film mass is less than was expected. This was explained by water exclusion induced by cation−proton exchange. Our findings suggest the same type of behavior, and we conclude that the negative value of the first fractional coefficient is actually caused by water desorption.

The glass transition temperatures for Nafion in either the acid- or sodium-exchanged forms are significantly different[26,27] than that at which we perform measurements (25 °C) and, thus, we do not expect any large influence of them on our experimental results.

Curves 1, 2, and 3 in panel B of Figure 6 are plots for the individual terms in eq 6. The first (Fickian term) resembles a parabolic dependence in time, whereas curves 2 and 3 (relaxations) have sigmoidal shape. Curves 1 and 2 are to some extent symmetrical around zero value. This should be the case because bpy penetration and water desorption are time-dependent processes; each penetrant bpy molecule might be causing exclusion of tens of water molecules from the polymer network.[25] Even if the overall measured bpy absorption process in Figure 6A is a non-Fickian two-stage mechanism, the inset in panel B (the sum of the curves 1 and 3 actually represents bpy diffusion isolated from water desorption) shows a nearly parabolic shape that is characteristic of a Fickian diffusion mechanism.

The possibility that two processes each with positive going curves are superimposed (the faster one describing bpy diffusion into fluorocarbon domains and the slower representing bpy diffusion into ionic domains) is contrary to experiment and unable to produce the segment of the experimental curve with zero slope. Therefore, we concluded that, most likely, the difference in thickness and refractive index dynamics cannot be related to Nafion internal structure per se but rather to bulk transport processes.

An estimation of the bpy concentration in the Nafion films equilibrated with $3 \times 10^{-3}$ M solution was done in an experiment that involved two films of equal thickness, one soaked in $3 \times 10^{-3}$ M bpy in 0.1 M NaCl, the other in 0.1 M NaCl (the latter was used as a blank for a normal incidence absorbance measurement). Both films were identically prepared

and soaked overnight in appropriate solutions. The films were dried for 24 h under ambient conditions, and then the thickness and absorbance of each were measured. A solution calibration curve with several known concentrations was used to measure the solution molar extinction of bpy at 280 nm ($\epsilon_{280} = 1.33 \times 10^4$ $M^{-1}cm^{-1}$). In the Nafion film, the absorbance maximum was red-shifted ($\lambda_{max} = 298$ nm). Using the solution molar extinction, the measured dry film thickness, the measured normal incidence absorbance, and by assuming Lambert−Beer behavior, we estimated the concentration of bpy in the dry Nafion film to be $0.33 \pm 0.06$ M at equilibration (preconcentration factor, 110).

*3.4.2. Equilibration of bpy-Loaded Nafion in $1 \times 10^{-5}$ M $Fe^{2+}$ in NaCl Solution.* Partitioning of an $Fe^{2+}$ ($Fe^{2+}$ shows weak optical absorption in near-IR and near-UV) into a chemically selective film, followed by formation of a highly colored complex, caused substantial changes in the film optical constants. Our studies focused on the complexation reaction that occurred in the film between absorbed 2,2′-bipyridine and film ferrous ions. The spectrum of the $Fe(bpy)_3^{2+}$ complex in solution is shown as an inset in Figure 2. The time-dependent behavior of the bpy-loaded Nafion film upon exposure to $Fe^{2+}$ solution introduces three unknown physical parameters that vary in time (film thickness, refractive index, and extinction coefficient), and they cannot be modeled simply by using the Cauchy normal dispersion equation. Instead, a global optical model was constructed with a range of oscillators positioned at certain wavelengths (energies) to quantitatively describe the $Fe(bpy)_3^{2+}$ absorption spectrum in the film (Supporting Information).

The refractive index variation in time during complexation of $Fe^{2+}$ in the film is shown in Figure 7A. The dashed line corresponds to the refractive index of the Nafion film equilibrated only with the bpy ligand. Interesting behavior is observed on exposure of the film to $Fe^{2+}$ solution. First, the refractive index of the film abruptly decreased for approximately the first 30 min, and then it started to increase at certain wavelengths. This behavior is illustrated at three wavelengths in Figure 7B. Whereas the refractive index at 460 nm shows a constant decrease (wavelength region before the strong absorption band of the complex), the indices at 540 and 700 nm (after the absorption band maximum) first abruptly decrease and then increase until leveling off at about 150−200 min. According to anomalous dispersion, if the oscillator strength with an infinitely small broadening term is increased in time, the refractive index wavelength-dependent profile magnitude must increase at all wavelengths longer than the oscillator position in the spectrum and decrease at shorter wavelengths.[28] Obviously, this was not fulfilled through complexation; additional phenomenon must be taken into consideration.

The corresponding increase in the film extinction coefficient induced by complexation is shown in Figure 7C. Figure 7D represents the dynamics of the extinction coefficient at three selected wavelengths, documenting the time profile of the chemical reaction in situ. The set of equations:

$$I = I_0 \exp^{-\alpha b}$$

$$k = \frac{\lambda}{4\pi}\alpha \qquad (7)$$

$$A = \log \frac{I_0}{I} = \epsilon bc$$

where $\alpha$ is absorption coefficient, $b$ is film thickness, and $A$ is absorbance, was used to calculate the $Fe(bpy)_3^{2+}$ concentration at equilibrium. The Lambert−Beer law was assumed. On the basis of the additional assumption that the only absorbing species at 520 nm was the complex itself, the following expression for

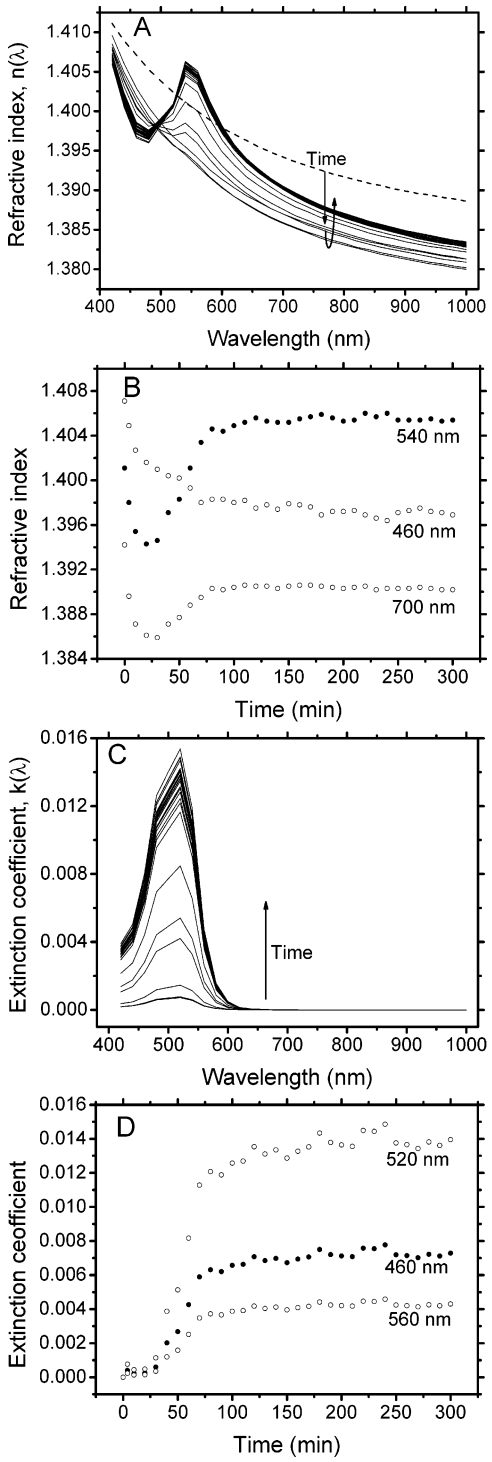


**Figure 7.** Panel A: film refractive index $n(\lambda)$ vs wavelength as a function of time for a Nafion film previously preconcentrated in $3 \times 10^{-3}$ M 2,2′-bipyridine during soaking in $1 \times 10^{-5}$ M $Fe^{2+}$ in 0.1 M NaCl solution. The dashed line denotes the refractive index of the film equilibrated in $3 \times 10^{-3}$ M 2,2′-bipyridine. Panel B: dynamics of the refractive indices at the three selected wavelengths. Panel C: film extinction coefficient vs wavelength for the Nafion film previously equilibrated in $3 \times 10^{-3}$ M 2,2′-bipyridine during soaking in $1 \times 10^{-5}$ M $Fe^{2+}$ in 0.1 M NaCl solution. Panel D: dynamics of the extinction coefficients at the three selected wavelengths (before, in proximity, and after absorption band maximum).

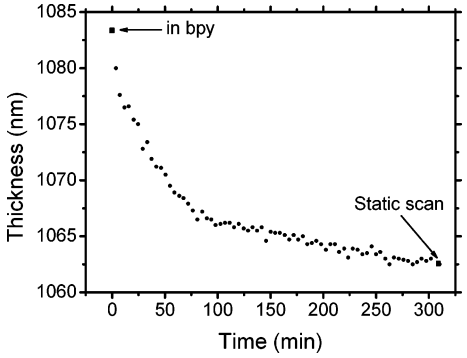


**Figure 8.** Film thickness vs time for the Nafion film previously equilibrated in $3 \times 10^{-3}$ M 2,2′-bipyridine during soaking in $1 \times 10^{-5}$ M $Fe^{2+}$ in 0.1 M NaCl solution.

concentration was obtained:

$$c = \frac{4\pi k_{520} \log 2.718}{\lambda_{520}\epsilon_{520}} \tag{8}$$

The $k$ value used in the calculation was obtained from the static mode scan ($k_{520} = 0.0145$). The calculated value of 0.19 $\pm$ 0.06 M is in reasonable agreement with the bpy concentration (0.33 M), bearing in mind the 1:3 stoichiometry of complexation and the experimental error in the determination of the concentration.

Interestingly, the film contracts as $Fe^{2+}$ partitions into and complexes with the bpy ligand, and this is shown in Figure 8. This contraction is probably partially due to electrostatic attraction between the charged complex and the $SO_3^-$ groups of Nafion and additional leaching of bpy molecules from the film. The fast changes are practically complete after 75 min, and starting from here, the film slowly equilibrated until the 300-minute mark. Excellent agreement between the static scan thickness and the dynamic scan value can be seen.

Prior to in situ metal−ligand complexation, we soaked the film in two steps: first, in 0.1 M NaCl solution where we expect that Nafion became deprotonated via proton/$Na^+$ exchange, and second, in ligand (bipyridine) solution. Because Nafion microstructure is well-explored and well-known (hydrophobic-fluorocarbon and hydrophilic-sulfonic acid group domains), it is reasonable to expect that Na ions occupy the hydrophilic domains and the ligands occupy the hydrophobic domains because of their high lipophilic character. In situ complexation in the final step requires that iron(II) ions migrate to the hydrophilic domains where they can complex with the ligand (presumably at the interface of the hydrophilic and hydrophobic domains) and form the charged $Fe(bpy)_3^{2+}$ complex. To fulfill charge, two further processes seem plausible: either two Na ions have to diffuse out of the hydrophilic domains, leaving the sulfonate groups bare and able to be neutralized by a metal−ligand complex, or the chlorides and/or iron solution counterions from the solution could screen the excess positive charge. We are not able with ellipsometry to prove or disprove either of these plausible processes.

The initial refractive index decrease can be explained in terms of some bpy initially leaching quickly out of the film that is driven by the high concentration gradient of bpy at the film/solution interface (vide supra). Apparently, the weak (presumably van der Waals) forces that bind bpy in the film are not strong enough to prevent some amount of leaching. The destiny of the leached ligand molecules cannot be easily predicted, but some of the expected events are: the bpy ligand could travel deeper in the bulk solution and can be lost for iron detection,

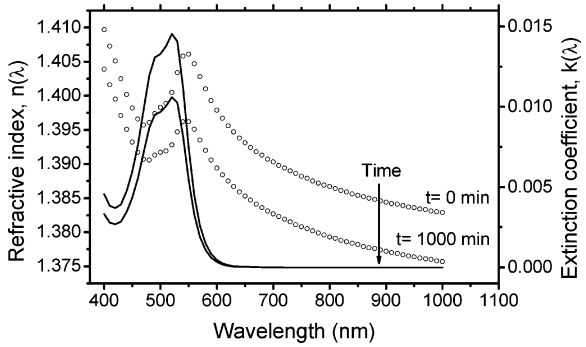


**Figure 9.** Leaching of $Fe(bpy)_3^{2+}$ complex from the Nafion film expressed by extinction coefficient and refractive index decrease during 1000 min soaking in 0.1 M NaCl solution. Dots correspond to refractive index, and solid lines to extinction coefficient.

or it could be complexed with iron in the vicinity of the film/solution interface and then either attracted back into the film by electrostatic interaction or diffused deeper in the solution.

*3.4.3. Stability of the Fe(bpy)$_3^{2+}$−Nafion Film System.* The $Fe(bpy)_3^{2+}$-equilibrated Nafion film in $Fe^{2+}$ solution was studied further. Calculation shows the dominant film chemical species to be the iron−bpy complex and this is consistent with the known high formation solution constant, $\log K = 17.2$ at room temperature.[29] At this point, the film was exposed to fresh circulating 0.1 M NaCl solution and the optical constants of the system determined. The results are sketched out in Figure 9, where the refractive index and extinction coefficient are plotted out as a function of wavelength for the two extremes of time. A clear indication of $Fe(bpy)_3^{2+}$ leaching out of the film is indicated by the decrease in the film extinction coefficient at the absorption maximum. In turn, leaching of the iron complex and possibly free $Fe^{2+}$ and bpy contribute to the general decrease with wavelength in the refractive index. From these data, one can estimate the percent iron complex leached after 1000 min, and it is quite significant (~30%), indicating a loosely bound ion-exchanged species More extensive leaching is apparently prevented by both electrostatic interaction between the charged complex with the negatively charged $SO_3^-$ groups in Nafion and weak hydrophobic forces that still exist for the complex and Nafion.

## 4. Conclusions

The usefulness of dynamic spectroscopic ellipsometry in understanding thin polymer film dynamics has been demonstrated by examination of a film-based chemical reaction. By using a prototype sensor system composed of a thin Nafion film on a glass substrate and spectroscopic ellipsometry, we have been able to quantitatively describe film-based processes that occur when a ligand-loaded film was exposed to complexing aqueous iron(II). Those processes have been partially isolated by a stepwise examination of component processes, ranging from initial film hydration and film loading with ligand bpy to the complexing of iron(II) with bpy ligands sorbed within the film. The loading of the hydrated Nafion film with the bpy ligand displayed a complicated kinetic that could be described by using an adaptation of the Berens−Hopfenberg two-stage diffusion model. The diffusion constant of bpy in the film obtained was in reasonable agreement with other reports of film diffusion constants. However, it is to be emphasized that detailed justification of using this model has not been done. In this context, it is not clear why water desorption was modeled by a sigmoidal relaxation term rather than a diffusion term. The

numerical success of the model used might reside in the similarity of the two types of functions (sigmoidal vs parabolic).

The results of the modeling suggested a two-stage polymer response to the ligand loading complimented by the expulsion of water from the film. Thus, our results are consistent with those previously that pointed to water sorption and desorption being important in hydrated Nafion film dynamics.[25] Although the bpy ligand was reversibly sorbed onto Nafion and would slowly leach out when exposed to continuously circulating fresh aqueous electrolyte, it is remarkable how stable the bpy-Nafion film is. When a bpy-loaded Nafion film was exposed to solution-phase $Fe^{2+}$, the film quickly incorporated the aqueous cation, presumably by ion exchange, and produced a film-bound highly colored $Fe(bpy)_3^{2+}$ complex. Indeed, it is surprising that, given the stoichiometry of the reaction and the lowered diffusion constants for film species, that the reaction occurs so efficiently in the film. The high association constant known for this metal complex apparently drives the film-based reaction to near completion. On the other hand, the complex is reversibly bound and was leached out of the film more readily than the ligand itself. We have not been able to identify any solution phase $Fe(bpy)_3^{2+}$, in all probability because the absolute amounts of the complex in one liter of circulating liquid is quite small.

Practical conclusions of this work are: (1) thin Nafion films prior to sensing aqueous iron should be loaded from solution with the bpy ligand for at least 15 h, realizing that the optimum equilibration time is thickness dependent in order to achieve the lowest possible detection limit, (2) leaching of the bpy ligand after introduction of the loaded film into a target analyte solution attenuates performance in a negative manner but not as much as one might expect given the reversible sorption of the ligand by the film, (3) the iron(II)−ligand complex formed within the film was highly chemically stable, and this has the net effect of driving solution phase iron(II) into the film, and (4) the inclusion of iron(II) itself into a hydrated electrolyte-equilibrated Nafion film does not significantly change film properties.

**Acknowledgment.** Support from the Office of Environmental Management Sciences Program of the U.S. Department of Energy (Grant DE-FG0799ER62331) is greatly acknowledged. The purchase of the spectroscopic ellipsometer was made possible by a grant from the Hayes Fund of the State of Ohio. The first author (N.P.) was supported in part by an Ohio Board of Regents Doctoral Investment Award. We thank Dr. Imants Zudans for suggestions during manuscript preparation.

**Supporting Information Available:** Measurement of the optical constants for glass materials used in studies, the method for optical constant measurements on liquids, data table containing measured Cauchy coefficients for glass materials and solutions used in this work, overview of the optical modeling with oscillators when refractive index (dielectric function) was complex value ($k(\lambda) \neq 0$), table containing Tauc−Lorentz and pole oscillator parameters used to mimic $Fe(bpy)_3^{2+}$ extinction coefficient wavelength-dependent profile.[30,31] This material is available free of charge via the Internet at http://pubs.acs.org.

## References and Notes

(1) Maghasi, A. T.; Conklin, S. D.; Shtoyko, T.; Piruska, A.; Richardson, J. N.; Seliskar, C. J.; Heineman, W. R. *Anal. Chem.* **2004**, *76*, 1458−1465.
(2) Shtoyko, T.; Conklin, S.; Maghasi, A. T.; Richardson, J. N.; Piruska, A.; Seliskar, C. J.; Heineman, W. R. *Anal. Chem.* **2004**, *76*, 1466−1473.
(3) Richardson, J. N.; Dyer, A. L.; Stegemillar, M. L.; Zudans, I.; Seliskar, C. J.; Heineman, W. R. *Anal. Chem.* **2002**, *74*, 3330−3335.
(4) Shtoyko, T.; Richardson, J. N.; Seliskar, C. J.; Heineman, W. R. Spectroelectrochemical Sensing Based on Multimode Selectivity Simultaneously Achievable in a Single Device. 14. Enhancing Sensitivity of a Metal Complex Ion by Ligand Exchange, *Electrochim. Acta* **2005**. In press.
(5) Greef, R. *Thin Solid Films* **1993**, *233*, 32−39.
(6) Christensen, P.; Hamnett, A. *Electrochim. Acta* **2000**, *45*, 2443−2459.
(7) Hamnett, A. *J. Chem. Soc., Faraday Trans.* **1993**, *89*, 1593−1607.
(8) Zudans, I.; Seliskar, C. J.; Heineman, W. R. *Thin Solid Films* **2003**, *426*, 238−245.
(9) Zudans, I.; Heineman, W. R.; Seliskar, C. J. *J. Phys. Chem. B.* **2004**, *108*, 11521−11528.
(10) Zudans, I.; Heineman, W. R.; Seliskar, C. J. *Chem. Mater*. **2004**, *16*, 3339−3347.
(11) Piruska, A.; Zudans, I.; Heineman, W. R.; Seliskar, C. J. *Talanta*. In press.
(12) Tompkins, H. G.; Smith, S.; Convey D. *Surf. Interface. Anal.* **2000**, *29*, 845−850.
(13) Tompkins, H. G.; McGahan, W. A. *Spectroscopic Ellipsometry and Reflectometry*, John Wiley & Sons: New York, 1999.
(14) Zudans, I. In Situ Studies of Sensor Film Dynamics by Spectroscopic Ellipsometry. Ph.D. Thesis, University of Cincinnati, Cincinnati, OH, August 2003.
(15) Tiwald, T. E.; Thompson, D. W.; Woollam, J. A.; Pepper, S. V. *Thin Solid Films* **1998**, *313−314*, 718−721.
(16) Palik, E. D. *Handbook of Optical Constants of Solids*; Academic Press: San Diego, 1998.
(17) Crank, J. *The Mathematics of Diffusion*, 2nd ed.; Clarendon Press: Oxford, New York, 1975.
(18) Filipov, L. K. *J. Chem. Soc., Faraday Trans.* **1993**, *89*, 4053−4057.
(19) Tang, Y.; Lu, J. R.; Lewis, A. L.; Vick, T. A.; Stratford, P. W. *Macromolecules* **2002**, *35*, 3955−3964.
(20) Berens, A. R.; Hopfenberg, H. B. *Polymer* **1978**, *19*, 489−496.
(21) Kristensen, E. W.; Kuhr, W. G.; Wightman, R. M. *Anal. Chem.* **1987**, *59*, 1752−1757.
(22) Buttry, D. A.; Anson. F. C. *J. Am. Chem. Soc.* **1983**, *105*, 685−689.
(23) Martin, C. R.; Rubinstein, I.; Bard, A. J. *J. Am. Chem. Soc.* **1982**, *104*, 4817−4824.
(24) Samec, Z.; Trojánek, A.; Samcová, E. *J. Electroanal. Chem*. **1995**, *388*, 25−34.
(25) Shi, M.; Anson, F. C. *J. Electroanal. Chem*. **1996**, *425*, 117−123.
(26) Yeo, S. C.; Eisenberg, A. *J. Appl. Polym. Sci*. **1977**, *21*, 875−898.
(27) Kyu, T.; Eisenberg, A. *Mechanical Relaxations in Perfluorosulfonate Ionomer Membranes*; ACS Symposium Series 180; American Chemical Society, Washington DC 1982; pp 79−110.
(28) Fowles, G. R. *Introduction to Modern Optics*, 2nd ed.; Dover Publications: New York, 1989.
(29) Martell, A. E.; Smith, R. M. *Critical Stability Constants*; Plenum Press: New York, 1989.
(30) Jellison, G. E., Jr.; Modine, F. A. *Appl. Phys. Lett*. **1996**, *69*, 371−373.
(31) Azzam, R. M. A.; Bashara, N. M. *Ellipsometry and Polarized Light*; Elsevier: Amsterdam, 1987.